



3 1176 00091 1710

NATIONAL ADVISORY COMMITTEE FOR AERONAUTICS

TECHNICAL MEMORANDUM 1300

WIND-TUNNEL CORRECTIONS AT HIGH SUBSONIC SPEEDS PARTICULARLY FOR AN ENCLOSED CIRCULAR TUNNEL

By B. Göthert

Translation

“Windkanalkorrekturen bei hohen Unterschallgeschwindigkeiten unter besonderer Berücksichtigung des geschlossenen Kreiskanals.”
Forschungsbericht Nr. 1216, Deutsche Versuchsanstalt für Luftfahrt,
E. V., Institut für Aerodynamik, Berlin-Adlershof, May, 1940.



Washington

February 1952

NATIONAL ADVISORY COMMITTEE FOR AERONAUTICS

TECHNICAL MEMORANDUM 1300

WIND-TUNNEL CORRECTIONS AT HIGH SUBSONIC SPEEDS

PARTICULARLY FOR AN ENCLOSED CIRCULAR TUNNEL*

By B. Göthert

SUMMARY

After a review of existing publications on wind-tunnel corrections at high Mach numbers, an approximate method is given for determining the corrections due to model displacement and wake displacement behind resistance bodies and due to the lift. The correction computations are first carried out for the incompressible flow. According to the Prandtl principle, the models and the wind tunnels in the incompressible flow are made to correspond to the models and the wind tunnels in the compressible flow; between the corrections of these two correlated tunnels definite relations then exist. Because of the Prandtl principle is applied only to the flow at a large distance from the models, the wind-tunnel corrections can also be computed if the assumptions in the Prandtl principle are not satisfied in the neighborhood of the model. The relations are investigated with particular detail for fuselages and wings of various spans in closed circular tunnels. At the end of the report a comparison is made between the computations and the tests in the DVL high-speed wind tunnel.

I. STATEMENT OF PROBLEM AND REVIEW OF LITERATURE

If a model of finite thickness is mounted in a closed tunnel, the tunnel at the model cross section is narrowed by a definite amount because of the displacement of the model. The air is now forced by this contraction to flow around the model with greater velocity than would be the case in an unlimited air stream. In the application of the results of measurement to the free air stream, the measured values are therefore to be correlated with a higher velocity than corresponds to the velocity in the tunnel without the model.

*"Windkanalkorrekturen bei hohen Unterschallgeschwindigkeiten unter besonderer Berücksichtigung des geschlossenen Kreiskanals." Forschungsbericht Nr. 1216, Deutsche Versuchsanstalt für Luftfahrt, E. V., Institut für Aerodynamik, Berlin-Adlershof, May, 1940.

For wind tunnels with small velocities, as have so far been predominantly used, the increase of the velocity due to the model is so small in view of the generally small model dimensions that it may generally be neglected. For higher tunnel velocities the velocity correction increases very rapidly, however, and at a more rapid rate the more nearly the velocity approaches that of sound. This fundamental behavior is shown, for example, by Ferri (reference 1, p. 112) by computing the velocity increase due to a definite amount of tunnel narrowing on the assumption of a uniform velocity distribution over the narrowed cross section (see fig. 1). From these computations it is found, for example, that a narrowing by the model of the tunnel by 1 percent gives, at small Mach numbers, an increase in velocity of 1 percent; for the Mach number $M = 0.8$, 2.7 percent; and for $M = 0.90$, as much as 11.0 percent.

This simple rough computation indicates the absolute necessity, on the one hand, of computations for the correction of the tunnel velocity due to the model displacement and, on the other hand, the need for choosing the dimensions of the model in relation to those of the tunnel so as to be smaller the nearer the velocity of sound is approached.

Accurate computations for flows in a compressible fluid, on account of the complicated considerations, currently offer little promise of success when it is considered that even the simple case of the two-dimensional flow about a wing in an infinite compressible air stream already lies at the limit of present-day computation possibilities. Approximations must therefore be sought that come as close as possible to the actual facts.

1. Approximate Computation of Lamla

A simple estimate of the correction for two-dimensional flow was given by Lamla (reference 2), who in his computations took into account the compressibility of the air up to terms of higher order and made use of the following concept as a basis:

If a wing with infinite span is placed in an air stream (without lift), two streamlines lying symmetrical to the wing at a large distance ahead of and behind the wing are separated by a distance h_∞ , while in the plane of the wing they are displaced by the greater distance $h_\infty + \Delta h$. Between two streamlines at distance h_∞ therefore, the flow in the model cross section no longer transports the same quantity of air G_∞ as between the streamlines the same distance apart at a large distance ahead of or behind the wing, but a smaller quantity of air $G_\infty - \Delta G$. Lamla takes the approach velocity v in the free air

stream to be increased by the amount Δv_0 until at the model cross section between two streamlines at distance h_∞ the quantity G_∞ is transported. The required increase in the velocity is considered as an approximate value for the velocity correction to be applied to the closed tunnel; the distance between the two streamlines h_∞ are set equal to the distance between the tunnel walls.

An important result of this estimate of Lamla was that the velocity corrections given by Ferri were recognized as upper limiting values, which can be attained only for very slender models with very large chord in comparison with the tunnel diameter. In by far the majority of cases, however, the chord of the model is so small in comparison with the tunnel diameter and its thickness ratio so large that the disturbance velocities produced by the model from the immediate neighborhood of the model up to the tunnel wall are greatly decreased and therefore also the effect on the flow produced by the wall becomes considerably smaller. For example, with 4 percent cross-sectional narrowing by the model, the velocity correction for the Mach number $M = 0.75$ is given by (from fig. 8 of reference 2):

Model	Thickness ratio, d/t	Velocity correction $\Delta v/v_0$ (percent)
Plate in direction of flow with finite thickness	$\rightarrow 0$	11.4 according to Ferri 11.4 according to Lamla
Elliptical cylinder	0.1	11.4 according to Ferri 4.2 according to Lamla

The numerical values found by Lamla, on account of the great simplification used, can only serve as guides for the approximate values of the corrections. The tunnel boundary conditions enter his computation only partly because equal flow was assumed through the cross section at the model position and the cross sections far ahead of and behind the model. This inexact taking into account of the effect of the tunnel wall led to the result that, in accordance with his computations for all Mach numbers, as for example for $M = 0$, the closed and the open tunnel have equal corrections of the velocity but with opposite sign. For compressible flow it is known, however, that the open tunnel requires only about one-half or one-fourth as large corrections as for the closed tunnel (reference 3, pp. 54-58).

2. Approximate Computation of Franke-Weinig

A further approximation for the two-dimensional problem is given by Franke and Weinig (reference 4). In their investigation they strictly consider the boundary conditions along the tunnel wall and take into account the compressibility in a manner similar to Prandtl. The velocity correction due to the displacement of the model is given in the following form:

$$\frac{\Delta v_x}{v_0} = \frac{F}{6} \frac{\pi}{h^2 (1-M^2)^{3/2}}$$

$$= \frac{1}{3} \left[\frac{1}{2}(v_{\text{above}} + v_{\text{below}}) - v_0 \right]$$

where

F	cross-sectional area of profile
h	distance of tunnel wall
v_{upper} and v_{lower}	velocity at upper and lower tunnel wall, respectively, in plane of model
v_0	velocity far ahead of model
$M = v/a$	Mach number, $\frac{\text{tunnel velocity}}{\text{velocity of sound}}$

The second form of the velocity correction given previously, which refers to the disturbance velocity measured at the wall, is in many cases found to be very useful. This form is referred to also in the following investigation (see section IV) in cases in which the assumptions of the Prandtl principle in the neighborhood of the model are no longer satisfied although, with the aid of the wall velocity, a correction according to the Prandtl principle is still possible.

3. Purpose of the Present Investigation

The purpose of the present investigation is to give a useful approximation of the velocity and angle-of-attack correction, in particular for the circular-shaped closed wind tunnel. Because at high Mach numbers the wake produced by the model resistance greatly increases, an approximation to take account of this wake is developed. Further, the results obtained are checked with the aid of wind-tunnel

measurements so far as the available measurements permit such comparison.

In contrast to the work so far done, the computation is first carried out completely for the incompressible flow. The results thereby obtained are applied to the flow in compressible media by correlating each flow picture of the compressible flow with a definite flow picture in the incompressible flow with suitably modified tunnel and model dimensions so that for both flow pictures the corrections are either the same or stand in definite relation to each other. This computation method has the advantage of great clarity of computation, for the investigation is split up into two independent partial investigations. Furthermore, a large number of already existing correction computations for incompressible flows can, according to the same principles, be applied in a simple manner to compressible flows so that a good portion of the existing data is not lost but can be further utilized.

The investigation was carried out in general form both for bodies of rotation and for wings of various spans. The numerical data given refer, however, predominantly to the case of the flow with rotational symmetry. In a further report that is soon to follow the numerical data will be supplemented.

II. CORRECTION OF THE FLOW VELOCITY DUE TO MODEL

IN CASE OF INCOMPRESSIBLE FLOW

1. Equivalent Dipole or Source Strength of Model

(a) Equivalent dipole strength of model without wake.

The flow about profiles or about bodies of arbitrary shape can, as is known, be simulated by definite arrangements of sources and sinks or of dipoles (doublets), the strength and distribution of which are so chosen that the resulting streamline coincides with the outline of the body investigated. For large distances from the dipole or source-sink system, the disturbance velocities produced by them can be shown to be equal to that of a single equivalent dipole that is located at the center of gravity of the system of singularities and whose strength is determined as follows¹:

Intensity of equivalent dipole

$$M^+ = 2 \sum (a Q) = \sum M$$

¹The equation given holds not only for doubly symmetrical but also for arbitrary body shapes.

where

Q strength of source or sink

2a distance between source and corresponding sink

M moment of elementary dipole

On the assumption that the dimensions of the model are small as compared with the diameter of the wind tunnel, the disturbance velocity of a model at the tunnel wall can be represented by the effect of the previously defined equivalent dipole M^+ . For large models, whose chord is comparable with the tunnel diameter, the simple estimate previously given of the equivalent dipole strength is insufficient; for this case a computation will later be given that permits estimating the deviation from the simple equivalent dipole.

The equivalent dipole for various shapes of bodies was computed by Glauert as a function of the maximum thickness and the ratio of thickness to length of the body (reference 3). In the present report, Glauert's results are so modified that the equivalent dipole strength becomes a function primarily of the volume of the displacing body; the effect of the thickness ratio and the difference between two-dimensional and three-dimensional flow then remain very small for slender bodies. In this new representation the dipole intensity is given by²:

²For cylinders, Glauert gives the equivalent dipole strength as

$$M^+ = \lambda \ b \ \pi/2 \ d_{\max}^2 \ v_0$$

(reference 3, p. 53). The given value referred to the volume λ_V is therefore connected with the λ value of Glauert by the relation

$$\lambda_V = \frac{\pi}{2} \frac{d_{\max}^2 b}{V} \ \lambda$$

For the circular cylinder, $\lambda = 1$ and therefore $\lambda_V = 2$. For bodies with rotational symmetry,

$$M^+ = \lambda \ \frac{\pi}{4} \ d_{\max}^3 \ v_0$$

(reference 3, p. 59) and therefore

$$\lambda_V = \frac{\pi}{4} \frac{d_{\max}^3}{V} \ \lambda$$

For the sphere, Glauert gives $\lambda = 1$ so that $\lambda_V = 1.5$.

$$M^+ = 2 \Sigma (a Q) = \lambda_V V v_0 \quad (1)$$

where

V volume of body

v_0 approach velocity

For bodies with rotational symmetry the equivalent dipole is to be applied at the center of gravity of the body. For cylinders ($t/b \rightarrow 0$) the previously computed equivalent dipole strength is to be distributed along the axis of gravity of the cylinder so that along this axis there is a uniform dipole distribution $dM^+ = db M^+/b$

The factor λ_V depends on the shape of the body and the thickness ratio. For very slender bodies ($d/t \rightarrow 0$) in two-dimensional and rotational symmetry cases, λ_V has the same value $\lambda_V = 1$.

For bodies with elliptical outline, the factor λ_V is given in figure 2 as a function of the thickness ratio for the two limiting cases of rotational symmetrical bodies and elliptical cylinder ($t/b \rightarrow 0$). It is seen from the figure that, for slender bodies such as occur in airplane structures, λ_V differs only by a slight amount from unity, for example,

$$\text{wing with } d/t = 0.15 \quad \lambda_V = 1.15$$

$$\text{fuselage with } d/t = 0.25 \quad \lambda_V = 1.065$$

For the very thin plate transverse to the air stream, the volume of the body is zero. Because, however, such a plate will nevertheless give a displacement of the streamlines, the factor λ_V must tend to infinity. If the computations in the literature³ are used for the flow about a plate, the product is obtained for the plate with constant height h and very large span b ($h/b \rightarrow 0$):

$$\lambda_V V = \frac{\pi}{4} h^2 b$$

and for the circular disk with the diameter d :

$$\lambda_V V = \frac{1}{\pi} d^3$$

³For very wide plate: reference 5. For circular plate: reference 6.

(b) Equivalent source strength to take into account the
wake displacement behind a drag body

Behind bodies which a flow drag connects with an energy loss (but not an induced drag), as is known, a wake or dead-water region is formed that evidently increases the displacement of the body. (See fig. 3.) This dead-water region has its source in the neighborhood of the body and extends downstream to infinity, with increasing mixing with the normal flow. It is useful to represent the effect of this dead water for points at a great lateral distance away by a system of sources that arise at the place of the drag body and displace the normal stream behind the body by the same amount as the wake. Between the strength Q of this source system and the drag of the body, under certain simplifying assumptions, a relation can be given which may serve as an estimate for the displacement due to the wake⁴.

⁴According to the momentum theorem, if the undisturbed pressure is assumed to prevail at the cross section considered behind the body, the drag W of a body is given by

$$\begin{aligned} W &= \int dm \Delta v = \text{mass flow per second} \times \text{velocity loss} \\ &= \rho \int (v_0 - v_1) v_1 df = \rho \int \left[(v_0 - v_1) v_0 - (v_0 - v_1)^2 \right] df \\ &= \sim \rho v_0 \int (v_0 - v_1) df \end{aligned}$$

(See fig. 3.) The integral contained in the last equation gives, however, precisely the additional strength per unit volume Q of the equivalent source that, on the assumption of potential flow, displaces the streamlines at a great lateral distance from the wake by the same amount as the wake, that is,

$$Q = \int (v_0 - v_1) df \quad \text{or} \quad W = \sim \rho v_0 Q$$

By transformation

$$Q = \frac{W v_0}{\rho v_0^2} = f_{ws} v_0 / 2$$

is obtained. The same relation between the source strength and the drag has already been given by reference 7 (p. 32).

On the assumption that the static pressure in the wake differs only slightly from the pressure of the undisturbed flow, there is obtained, by neglecting small quadratic terms, equivalent source strength:

$$Q = \frac{1}{2} v_0 f_{ws} \quad (2)$$

where $f_{ws} = c_w F$ represents the harmful drag of the body (without account taken of the induced drag). This relation between the source strength and the drag area is independent of the shape of the body and holds both for two-dimensional and for three-dimensional flow.

The exact location of this equivalent source is not uniquely determined. It appears admissible, however, to assume the source as located at the center of gravity of the volume. Although the position of the equivalent source may not be correctly given by this assumption, the error thus introduced is small provided that the equivalent is used only to represent the flow relations at a great distance from the source. This assumption is, however, satisfied for obtaining the tunnel corrections because the model dimensions are always small in comparison with the tunnel diameter.

In the derivation of the preceding equivalent source strength, the assumption was made that the static pressure in the wake differed only slightly from the pressure of the undisturbed stream. At a large distance behind the drag body this assumption holds quite well, so that to a very good approximation the previously given equivalent source strength remains the same although the dead-water region constantly expands. Immediately behind the wing, however, the static pressure may differ greatly from the undisturbed pressure of the flow so that deviations from the simple relation given above between the drag and the source strength are obtained. It was shown by Muttray that the source strength decreases rapidly from a maximum value at the wing trailing edge to a final constant value behind the wing (reference 7, fig. 22). This decrease means, however, that, to the previously computed equivalent source strength, a system of additional sources and sinks behind the wing is to be added. At a large distance from the wing, as for example at the tunnel wall, this additional source system acts approximately like a single dipole. The action of this additional wake dipole is taken into account in the following correction computations if the magnitude of the tunnel corrections from the disturbance velocities measured at the wall is determined according to equation (4). The error made in assuming that the location of this wake dipole does not coincide with the profile center of gravity is only of small significance on account of the effect of the wake corrections.

The same consideration applies also to the additional displacement due to the compression shocks, so that their effect can enter approximately into the corrections provided the shock length is small as compared with the tunnel diameter.

2. Disturbance Velocity at the Tunnel Center and at the Wall

Due to the Model and the Dead Water

Because, according to the assumption made, the model dimensions are small in comparison with the tunnel diameter, the disturbance velocities at the tunnel wall can be represented by the previously determined equivalent dipole and the equivalent source. The boundary condition which is to be satisfied by the presence of the tunnel wall for the closed tunnel is that all velocity components normal to the tunnel wall must vanish.

This requirement is satisfied, as is known, by superimposing an auxiliary flow with a velocity field on the flow about the model in the free airstream so that the composite flow satisfies the previously given condition. The computation for the circular tunnel is quite complicated. In the present case the solution was determined by a method given in reference 8 (p. 250) of developing the field of the radial velocities along the tunnel wall and the velocity field of the auxiliary flow into a Fourier series. By comparing the coefficients of the two Fourier series, the constants for the velocity field of the auxiliary flow were then obtained so that the velocity at arbitrary points of the flow field could be determined. As velocity correction, that velocity is taken which induces the auxiliary flow at the location of the model.

The results of this computation are given in the present report for the additional velocities at the tunnel center and for the symmetrical case (with the equivalent dipole and equivalent source at the tunnel center) and for the additional velocity at the tunnel wall, because for these arrangements the computation is still relatively simple, only the first term of the Fourier series being taken into account. For several nonsymmetrical arrangements with respect to the excess velocity at the tunnel wall, numerical values are also given for which the first four Fourier terms entering the computation were taken into account. It is still necessary to check whether the further Fourier terms have an effect on the results⁵.

⁵A further report will be issued on the required corrections of the given numerical data when the higher Fourier terms are taken into account in which the computation procedure will also be described in detail.

(a) Disturbance velocity due to the model.

In the notation of Glauert, the velocity correction to be applied at the tunnel center is written as follows:

$$\frac{\Delta v_x}{v_0} = \tau_V \lambda_V \frac{V}{D^3} \quad (3)$$

where

V volume of body

D tunnel diameter

As has been previously explained, λ_V represents a factor that takes into account the model shape. (See fig. 2.) The factor τ_V depends on the tunnel shape and on the ratio of the model dimensions to the tunnel diameter. For a closed circular tunnel the factor τ_V is given in table 1 for several typical cases.

In the method given by Weinig, the additional velocity at the center of the tunnel may also be represented as a function of the additional velocity at the wall of the tunnel. As in the two-dimensional case computed by Weinig, it may also be shown for the closed circular tunnel that the disturbance velocities occurring at the plane of the model at the tunnel wall Δv_{xw} due to the model bear a definite ratio to the disturbance velocity Δv_x at the tunnel center. (See fig. 4.) If, for the comparison velocity Δv_{xw} , the arithmetical mean of the velocities above and below the model is chosen, this mean value is independent of the lift because a potential vortex at the model at these two points induces equal but opposite circulation velocities. The wall velocity, according to figure 4, is composed of two parts: namely, a part that directly represents the disturbance velocity of the equivalent dipole and a part that is due to the wall effect. The required velocity Δv_x at the tunnel center may therefore be written as

$$\frac{\Delta v_x}{v_0} = m \frac{\Delta v_{xw}}{v_0} \quad (4)$$

The factor m in this equation depends on the tunnel shape and on the ratio of the model dimensions to the tunnel diameter. For the closed circular tunnel the factor m for several typical cases is given in table 2.

For comparison, it may be mentioned here that for a wing with infinite span between two walls, Weinig gives the value $m = 1/3$. The factor m is likewise found to depend to a relatively large degree on the tunnel shape.

(b) Correction for models of very large chord

The numerical values given in the preceding section (a) for the velocity corrections were computed on the assumption that all the model dimensions except the wing span were small compared to the tunnel diameter. It is often necessary, however, to obtain an idea of how the data are modified if the preceding assumption no longer holds true with respect to the model chord.

In order to investigate this effect on bodies of rotation in the center of the tunnel, the additional velocities at the tunnel center and at the wall were computed for various distances of the source-sink system replacing the body by the method given in section (a). The distribution of the sources and sinks for these bodies was chosen as shown in figure 5. With this arrangement, the ratio F_{profile}/d was found to be equal to 0.75 as corresponds to the usual shapes in airplane structures and to wings and fuselages. Because for these bodies the magnitude of the equivalent dipole is known from equation (1) $M^+ = \sum (2aQ)$, the disturbance velocities at the center of the tunnel and at the wall can likewise be immediately given by equations (3) and (4) if the effect of the large model chord is neglected. Through a comparison of the results, the numerical values for T_v and for the ratio m (equations (3) and (4)) were found to require a correction. The correction is represented in figure 6. For very large model chord, the additional velocities at the tunnel center are seen to differ only by a small amount from the value for vanishingly small models. The wall velocity Δv_{xw} and therefore also the ratio m of wall velocity to center velocity depend, however, to a great extent on the model chord. For example, for a wing whose chord is equal to the tunnel diameter, the center velocity is 89 percent of the velocity obtained on the assumption of vanishingly small model chord, whereas the wall velocity is 66 percent of the corresponding value.

The previous investigations for models of large chord refer only to bodies with rotational symmetry and to wings with vanishingly small span in comparison with the tunnel diameter. Strictly speaking, it would be necessary to carry out also corresponding computations for wings with various ratios of the span to the tunnel diameter. Before the results are extended in this respect, however, it may be assumed as a useful approximation that the correction values given in figure 6 hold also for wings with finite ratio of span to tunnel diameter.

(c) Disturbance velocity due to the wake

The effect on the tunnel wall of the dead-water region formed behind a drag body and therefore the effect on the tunnel correction can be given approximately by an equivalent source at the location of the model. (See section II, 1, (b).) If, for this flow, the boundary conditions at the tunnel wall are satisfied by superposition of the source flow in the free air stream on an additional velocity field according to section II, 2, (a), it is readily seen that in the closed tunnel at the model location no velocity component arises in the approaching flow direction because of the additional flow field; only for unsymmetrical arrangement of the source in the tunnel will a velocity component arise at right angles to the approaching flow direction, which leads to a change of angle of attack. This change of angle of attack is also, however, in general without significance, for models are practically never mounted unsymmetrically in the wind tunnel.

Although no velocity component in the the flow direction is induced by the additional velocity field at the model location, a correction for the approach velocity in the closed tunnel is necessary. The relations are seen most simply with the aid of figure 7 in the case of the infinitely wide tunnel. The velocity field arising from the source in the tunnel and from the external sources reflected in the wall is characterized by the fact that the velocity components in the model plane in the flow direction vanish. At an infinite upstream and downstream distance, however, a parallel flow is formed with the velocity $v = \pm \frac{1}{2} \frac{Q}{F_K}$. For the flow in the tunnel at a large distance from the source this means that the approach velocity is no longer v'_0 but $v_0 = v'_0 - \frac{1}{2} \frac{Q}{F_K}$. The velocity v_0 therefore increases up to the plane of the model by the amount $\Delta v_x = \frac{1}{2} \frac{Q}{F_K}$ and up to a section very far behind the body by $\Delta v = Q/F_K$. The required approach-velocity correction in the closed tunnel is, therefore, with the aid of equation (2), obtained as

$$\frac{\Delta v_x}{v_0} = \frac{1}{2} \quad \frac{Q}{F_K v_0} = \frac{1}{4} \quad \frac{f_{ws}}{F_K} \quad (5)$$

where

$f_{ws} = c_w F$ harmful drag area

F_K tunnel cross section

The distribution of this correction velocity over the model cross section is uniform; that is, at the tunnel center and at the wall there is the same velocity increment Δv_x . In the equation

$$\Delta v_x/v_0 = m \quad \Delta v_{xw}/v_0$$

the factor m therefore has the value $m = 1$.

This equation for the velocity correction due to the wake and magnitude of the factor m is independent of the shape of the closed tunnel and therefore holds for square as well as for circular tunnels, etc.

In a corresponding manner it may be shown simply that in wind tunnels with open test section no velocity correction is required to take into account the displacement due to the wake. The boundary condition of the free jet would be satisfied by reflecting sources and sinks alternately at the tunnel wall, in a similar manner to that indicated in figure 7. At the center of the tunnel no direct velocity component is obtained in the flow direction. At an infinite distance upstream and downstream of the plane of the source the velocity components due to the sources and the sinks reduce to zero as the velocities induced by them mutually cancel.

III. VELOCITY CORRECTION DUE TO THE MODEL AND THE WAKE AT

HIGH SUBSONIC VELOCITIES WITHIN THE REGION OF VALIDITY

OF THE PRANDTL PRINCIPLE

The equations given above for the tunnel correction hold only for the incompressible flow. With the aid of the Prandtl principle, however, a given tunnel with the model in a compressible flow can be correlated with another tunnel with models of modified dimensions in an incompressible flow. Between the velocities in the two corresponding tunnels definite relations hold so that, with the aid of these relations, the flow in the compressible medium can be reduced to the flow in the incompressible medium. The form of the Prandtl principle which is here used is as follows (reference 9):

At each point of the compressible flow the same potential holds as compared with the corresponding point of the incompressible flow and the same velocity in the flow direction (x-direction) with the velocities at right angles to this direction reduced by the factor $\sqrt{1-M^2}$. The corresponding points in the two flow fields are connected by the following relations:

$$x_{\text{incompr}} = x_{\text{compr}}$$

$$y_{\text{incompr}} = \sqrt{1-M^2} y_{\text{compr}}$$

$$z_{\text{incompr}} = \sqrt{1-M^2} z_{\text{compr}}$$

where

M Mach number, $\frac{\text{tunnel velocity}}{\text{velocity of sound}}$

1. Model Displacement

For a wing with large aspect ratio B/t in a closed wind tunnel, the potential field for incompressible flow is shown in figure 8. The model is assumed to be slender enough and to possess a sufficiently sharp leading edge that the Prandtl principle is satisfied along the entire profile contour. The profile contour is given by the boundary streamline of a definite source-sink arrangement so that the potential lines are continued to the interior of the surface enclosed by the boundary streamline. On the potential lines $\phi = \text{const}$ so that they must intersect the tunnel wall and the profile surface at right angles, for at these bounding surfaces no normal velocity components exist.

If this potential field is now transformed according to the Prandtl principle, that is, if the lines $\phi = \text{const}$ are separated farther apart in the y and z directions by the factor $1/\sqrt{1-M^2}$, and the x component is kept constant, a new potential field is obtained for the compressible flow. (See fig. 8.) In this distorted potential field, condition for the tunnel wall, namely, that all potential lines must be at right angles to the flow direction, can be seen to be satisfied along a new contour whose y and z coordinates are increased by the factor $1/\sqrt{1-M^2}$. For circular tunnels this satisfaction means, for example, that the diameter of the tunnel in the compressible flow is greater than the comparison tunnel in the incompressible flow in the ratio $1/\sqrt{1-M^2}$.

In the transformation according to the Prandtl principle the wing in the tunnel receives definite modifications. If, for the slender body, the assumption is made that, within the bounding potential line which replaces the profile, the potential lines may be replaced by their tangents at their points of intersection with the x -axis, it is seen that the inclination of this tangent becomes steeper in the ratio $1/\sqrt{1-M^2}$. This assumption means, however, that the stream lines in the neighborhood of the x -axis, as also in particular the bounding

stream, have flatter slopes dy/dx by the factor $\sqrt{1-M^2}$ than before the distortion. The profile shape determined by the bounding stream-line is therefore thinner after the distortion in the ratio $\sqrt{1-M^2}$. The span of the wing with large aspect ratio B/t is determined by the length of the segment with sources and sinks or dipoles distributed on it. This distance is likewise increased by the distortion in the ratio $1/\sqrt{1-M^2}$ so that the comparison wing in the compressible flow has a greater span in the ratio $1/\sqrt{1-M^2}$.

Because the profile section has, through the transformation, become more slender in the ratio $\sqrt{1-M^2}$ but the span has become larger in the ratio $1/\sqrt{1-M^2}$, the initial wing and the corresponding wing of the compressible flow have the same volume. It is also known for slender bodies of rotation that in the transformation according to the Prandtl principle their contour is, to a first approximation, unchanged so that in this case also the volume undergoes no change (reference 8).

Because in the Prandtl transformation the velocity components in the flow direction remain the same, a condition that holds also without restriction for the velocity components due to the model and the tunnel wall, the same corrections on the approach velocities are to be used for the bodies in the compressible flow as for a body transformed in the manner explained above in an incompressible flow in a tunnel reduced by the factor $\sqrt{1-M^2}$.

If, therefore, a model that at small velocities has the approach-velocity correction $\Delta v_x/v_0$ for small velocities is placed in a closed tunnel and the Mach number continuously increased, the velocity correction according to equation (3) increases in the ratio $1/(1-M^2)^{3/2}$, that is,

$$\left(\frac{\Delta v_x}{v_0}\right)_{\text{compr}} = \frac{1}{(1-M^2)^{3/2}} \left(\frac{\Delta v_x}{v_0}\right)_{\text{incompr}} \quad (6)$$

In the preceding relation, the factors τ_v and λ_v contained in equation (3) were assumed not to vary in the transformation according to the Prandtl principle. For λ_v a small displacement actually occurs that is due to the change in the effective thickness ratio. According to figure 2, however, λ_v depends only to a slight extent on the thickness ratio, so that the change in λ_v may in general be neglected without great error.

The factor τ_v does not vary as long as the model chord is small in comparison with the tunnel diameter. With increasing Mach number, however, the effective ratio of model chord to tunnel diameter rises as $1/\sqrt{1-M^2}$, because the model chord remains unchanged while the tunnel diameter becomes smaller by the factor $\sqrt{1-M^2}$. When the Mach number is increased, the question is thus raised of the correction of models with large chord in a closed tunnel. According to figure 6, the correction

of the factor τ_v can be estimated by letting the effective ratio of the model chord to the tunnel diameter increase by the factor $1/\sqrt{1-M^2}$.

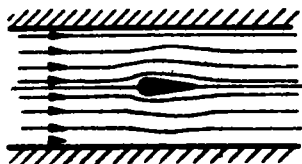
As long as the model chord can still be considered small in comparison with the tunnel diameter, the factor m in equation (3) undergoes no change. In the transformation according to the Prandtl principle, the same ratio of model span to tunnel diameter occurs for the comparison tunnel as for the initial tunnel, so that for both systems the same factor according to table 2 is to be used. If in the transformation too high ratios of chord to tunnel diameter result, however, then the value of m is to be corrected with the aid of figure 6.

2. Additional Velocity Due to the Wake

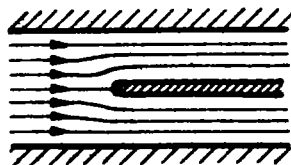
The same consideration for the computation of the velocity correction due to the model displacement can also be applied for the additional displacement due to the wake. In a purely formal manner, on the assumption that the drag surface does not vary with increasing tunnel velocity, there is obtained from equation (3):

$$\left(\frac{\Delta v_x}{v_0}\right)_{\text{compr}} = \frac{1}{1-M^2} \left(\frac{\Delta v_x}{v_0}\right)_{\text{incompr}} \quad (7)$$

It is thus seen that, in contrast to the cases so far given, the tunnel correction does not increase by $1/(1-M^2)^{3/2}$ but by $1/(1-M^2)$. Because, in this computation, the effect of the wake was replaced by the flow about a source which, as is known, gives in a parallel stream a bounding stream line in the form of a "half-body," the preceding result means that for a body of small chord, for example, a fuselage in a tunnel, the velocity corrections increase by the factor $1/(1-M^2)^{3/2}$; for a half-body in a closed tunnel the velocity corrections increase only by the factor $1/(1-M^2)$.



Fuselage in
tunnel



Half-body
in tunnel

The reason for this different behavior of the two body shapes is to be sought in the fact that for flow with rotational symmetry, the radial velocities acting on the wall at points a small distance upstream or downstream of the model for short bodies (equivalent dipole) decrease approximately in inverse ratio to the fourth power of the distance from the body, whereas for the half-body (equivalent source) they decrease only in the inverse ratio of the second power of the distance from the body. If, therefore, corresponding to the Prandtl principle, the tunnel

diameter in an incompressible flow is reduced for both bodies to the same extent, it is seen immediately that in the case of the half-body the wall effect must increase by a less amount than for the short body⁶.

If the velocity correction is again referred to the wall velocity, the factor m in equation (4) is still to be set equal to 1 for the region of validity of the Prandtl principle, because when the wake is taken into consideration, this factor is independent of the magnitude of the tunnel diameter. (See section II, 2, (c).)

IV. VELOCITY CORRECTION DUE TO THE MODEL AND THE WAKE FOR

THE CASE WHERE THE PRANDTL PRINCIPLE ALONG THE MODEL

SURFACE DOES NOT HOLD TRUE

The assumption for the validity of the Prandtl principle is that the additional velocities due to the body are small compared with the tunnel velocity. In many cases, particularly at high Mach numbers, this assumption is not satisfied along the surface of the body. At

⁶The radial velocities of source and dipole decrease according to these considerations, for small values of x , by the second or fourth power of R ; the additional velocities increase, however, with the second or third power of $1/\sqrt{1-M^2}$. This difference in the exponential relation is to be ascribed to the fact that at a great distance ahead of or behind the source and the dipole, the radial velocities in each case vary by the same amount so that an equalization of the power exponent occurs. A simple check computation for the amount of the velocity increase is possible for the half-body. If a half-body is in a closed tunnel, the stream is parallel far ahead of and behind its nose. The velocity increase is computed simply by the decrease in the cross section df . From the known equations

$$\frac{dp}{p} = k \frac{M^2}{1-M^2} \frac{df}{f}$$

and

$$\frac{dp}{p} = -kM^2 \frac{dv}{v}$$

in agreement with the relation previously found from the Prandtl principle:

$$\frac{dv}{v} = -\frac{1}{1-M^2} \frac{df}{f}$$

some distance ahead of or behind the body the additional velocities have become small enough, however, that for the flow outside of a definite boundary line the Prandtl principle may again be applied. (See references 10 and 4.) In figure 9, for example, the region enclosed by the boundary line no longer follows the Prandtl principles so that the transformation law is unknown for the streamlines within the boundary and for the body contour.

This fact is now applied to the flow in a tunnel, first for the simplest case of the flow in an infinitely wide tunnel with parallel walls. In an incompressible flow the boundary conditions at the tunnel wall are satisfied for the dipole replacing the body by an infinite reflection of the equivalent dipole at the tunnel wall. In the neighborhood of the dipole the disturbance velocities are so large, however, that within a certain limiting region the Prandtl principle is no longer applicable (fig. 10). The transformation of this incompressible flow field according to the Prandtl principle is possible, however, for the regions lying outside with boundary lines; within the boundary lines, as stated above, a transformation must be made according to an as yet unknown law so that the body contour for the compressible flow is likewise unknown. According to the Prandtl principle, the strength of the equivalent dipole can no longer be determined by computation for a given body. This gap can however be closed for the wind-tunnel test by a simple measurement. Because the additional velocity at the tunnel wall above and below the model is a measure of the effective dipole strength and the tunnel walls, moreover, lie within the region of validity of the Prandtl principle, the effective dipole strength can be determined by measuring the velocity at the wall. The required tunnel-correction velocity at the tunnel center, is as is known, the sum of the induced velocities of all reflected dipoles whose intensity is known from the measurement of the wall velocity and for which the tunnel center belongs to the region of validity of the Prandtl principle. This knowledge means, however, that between the wall velocity and the approach-velocity correction at the tunnel center the same relation holds as in an unrestricted region of validity of the Prandtl principle, that is,

$$\Delta v_x/v_0 = m \quad \Delta v_{xw}/v_0$$

This relation is not restricted to only the flow between two walls. As can be readily seen, it can be applied also for the closed tunnel of arbitrary cross-sectional shape, for example, for the circular tunnel. The only difference consists in the fact that in the flow between two walls the additional potential to satisfy the tunnel wall conditions is produced by the reflected singularities, whereas in the most general case the additional potential arises also from the

singularities outside of the tunnel; the strength and the location of these singularities cannot be found, however, by simple reflection.

As long as the model dimensions are small as compared with the tunnel diameter the values to be assigned to m are those given in table 2. For models with large chords and for high Mach numbers, however, an estimate for the correction of the factors m due to very large ratio of the chord of the model to the tunnel diameter must be made with the aid of figure 6.

The relations given between the velocity at the wall and the tunnel-correction velocity for flows about models, for which in the neighborhood of the model the Prandtl principle no longer holds, can also be derived for the velocities induced by the wake.

The previously described extension of the tunnel-correction computations to Mach numbers for which the Prandtl principle in the neighborhood of the model no longer holds is naturally inapplicable without restriction up to a Mach number $M = 1$. An upper limit of the applicability is given, for example, if the sound velocity is attained or exceeded at the tunnel wall. In this limiting case the assumptions of the Prandtl principle are no longer satisfied in the neighborhood of the tunnel wall so that the entire transformation process is inapplicable. How closely this upper limit may be approached in the wind tunnel measurement without fundamentally altering the pressure field about the profile can be determined by experiment. This limiting Mach number will depend, among other factors, on the degree of obstruction of the tunnel by the model and on the angle of attack of the model. Corresponding tests to determine admissible model dimensions for definite limiting Mach numbers and angles of attack are at present being conducted at the DVL.

V. TUNNEL CORRECTIONS DUE TO LIFT AT HIGH SUBSONIC VELOCITIES

1. Wing in Free Air Stream

In order to consider briefly the flow relations about a wing with lift in a compressible medium, the wing will first be considered replaced by a vortex filament in a free air stream. The flow field about a potential vortex in an incompressible flow is schematically represented in figure 11. If the velocities along the closed bounding line ABCD are added, the following integral represents the circulation of the vortex:

$$\oint v \, ds = Z = \text{circulation}$$

The magnitude of the circulation is, as is known, independent of the path of integration as long as the vortex lies within the boundary line. In a medium of constant density there is then obtained for the lift per unit length

$$A = \rho \quad Z \quad v_0$$

where ρ is the air density.

If the flow field of this vortex is now transformed according to the Prandtl principle where there is again excluded a region in the immediate neighborhood of the vortex center, the control surface ABCD is extended in the direction of the y axis. (See fig. 11.) At the same time, however, the velocity component v_y is reduced at corresponding points in the ratio $\sqrt{1-M^2}$ so that the product of the path element by the velocity at the normal boundary lines undergoes no change as a result of the transformation. Because, however, in the x direction neither the lengths nor the velocities have changed, the circulation integral along the lines ABCD or A'B'C'D' remains unchanged. If the line A'B'C'D' is taken at a very large distance from the vortex, where the disturbance velocities and therefore the pressure and density changes in the flow have been reduced to vanishingly small values, the compressible flow in the neighborhood of the control line completely resembles an incompressible flow, which means that for the lift per unit length the familiar relation again holds:

$$A = \rho \quad v_0 \quad Z$$

where ρ is the density of the medium at a great distance from the vortex.

From the preceding consideration, the conclusion can therefore be drawn that in the Prandtl transformation the circulation and the lift referred to the span element are unchanged.

For compressible flow the same lift per unit span is, as known, attained at an angle of attack reduced in the ratio $\sqrt{1-M^2}$. This is seen from the fact that in the transformation the velocity components normal to the flow direction become smaller while the components in the flow direction remain unchanged. The slope of the stream lines and therefore also the angle of attack thus become smaller in the same ratio.

The same considerations may be applied also for a wing of finite span with elliptical lift distribution. A wing in a compressible flow is then to be compared with a wing in an incompressible flow for which the span of the second wing is reduced in the ratio $\sqrt{1-M^2}$. At each

section at corresponding distances from the center of the wing the circulation and the lift per unit span element then agree for both wings with elliptical lift distribution, whereas in the incompressible flow the angle of attack, both the geometrical and the induced, are increased in the ratio $1/\sqrt{1-M^2}$. The comparison wing in the incompressible flow then has an aspect ratio (span b /chord t) impaired by the factor $\sqrt{1-M^2}$. For the induced drag in the compressible flow the equation

$$c_{wi} = c_a \quad \Delta\alpha_1 = \frac{c_a^2}{\pi} \frac{F}{b^2}$$

nevertheless still holds where

F wing area in compressible flow

b span in compressible flow

because for the comparison wing in the incompressible flow the induced angle of attack $\Delta\alpha_1$ is increased by $1/\sqrt{1-M^2}$ while through the transformation to a compressible flow this angle of attack is again reduced by $\sqrt{1-M^2}$. The two effects thus mutually cancel.

The equations for the induced angle of attack

$$\Delta\alpha_1 = \frac{c_a}{\pi} \frac{F}{b^2}$$

and the induced drag

$$c_{wi} = \frac{c_a^2}{\pi} \frac{F}{b^2}$$

retain their validity also for compressible flow.

2. Wing with Lift in the Wind Tunnel

As has already been stated in corresponding cases, a wing in the wind tunnel with compressible flow can be made to correspond to a definite wing with equal lift in a similar reduced wind tunnel with incompressible flow. Between the correction velocities of the comparison tunnel and the initial one the relation then exists that the v_y corrections in the compressible flow must be made smaller in the ratio $\sqrt{1-M^2}$. In this manner all correction computations can be carried over to the compressible flow.

The results of the existing wind-tunnel-correction computations are, in general, represented in the following form:

$$\text{Angle of attack correction: } \Delta\alpha = \delta \frac{c_a}{8} \frac{F}{F_K}$$

where

δ correction factor, function of ratio wing span to tunnel diameter, tunnel shape, and lift distribution

F wing area

F_K tunnel cross section

In the Prandtl transformation the value of the factor δ is not changed because the ratio of span to tunnel diameter, which determines its value, remains the same and so do the tunnel shape and the lift distribution. The wing area, however, becomes smaller in the ratio $\sqrt{1-M^2}$, the tunnel cross-sectional area in the ratio $(1-M^2)$ so that for the comparison tunnel in the incompressible flow the angle of attack is greater in the ratio $1/\sqrt{1-M^2}$. This increase is, however, again canceled in converting to the compressible flow because all v_y velocities and angles of attack become smaller in the Prandtl transformation by $\sqrt{1-M^2}$.

The important result is thus found that for elliptical lift distribution the angle-of-attack corrections and therefore also the corrections of the induced drag can be dealt with in the same way as for incompressible flow.

The assumption underlying the preceding general result is, however, that the dimensions of the wing with the exception of the span are small compared with the tunnel diameter and only the corrections at the location of the wing are considered. If such is not the case, as, for example, in the correction of a wing with large chord due to the stream curvature in the wind tunnel or in the computation of the downwash behind a wing, it is again advisable to make use of the idea of a comparison tunnel with its corrections determined. It is thus found, for example, that the correction due to the stream curvature for large chord wings increases as $1/\sqrt{1-M^2}$, the profile chord remaining the same in the Prandtl transformation, while the tunnel diameter becomes smaller by the factor $\sqrt{1-M^2}$. With increasing Mach number the ratios of the wing chord to the tunnel diameter also increase in the comparison. The corrections due to the flow curvature may therefore at high Mach numbers be of significance, although for an incompressible flow they may be entirely negligible.

VI. APPLICATION OF THE WIND TUNNEL CORRECTIONS DERIVED PREVIOUSLY

1. Superposability of the Individual Corrections

In the present work the different factors for the wind tunnel corrections, like model displacement, wake displacement, and lift, were treated as though only one of these magnitudes was alone effective (for example, a displacement body without lift and drag, or a lifting vortex without displacement, and so forth). In the wind tunnel test, however, the various factors enter in general together so that the question arises of the superposability of the individual corrections.

In the incompressible flow the question can immediately be answered in that the individual factors are simply to be superposed linearly. Each individual correction can, as is known, be computed from the corresponding potential field. Because for incompressible flow the potentials can be superposed linearly, the corrections derived from them can similarly be superposed linearly.

In the case of the compressible flow, a flow picture in the incompressible flow was made to correspond to each flow picture, with the aid of the Prandtl principle. Between the velocities and angles of attack of the two flow fields the familiar relations of the Prandtl principle hold. In the incompressible comparison flow field, the individual factors and the corrections may again be linearly superposed. Because the required corrections in the compressible flow differ from these comparison corrections only by a factor, the law of linear superposition of the corrections holds also for the compressible flow.

2. Application of the Corrections in the Wind-Tunnel Test

(a) The corrections due to the lift are obtained according to the known equations from the measured lift. The corrections do not increase, for equal lift coefficient, with increasing Mach number as long as the model chord in the comparison tunnel remains small as compared with the tunnel diameter. The corrections due to flow curvature for large-chord models increase, however, with increasing Mach number in the ratio $1/\sqrt{1-M^2}$ so that these corrections can become of significance although for the incompressible flow they are entirely negligible.

(b) The corrections due to the measured drag are computed according to equations (5) and (7). They increase for equal drag area $f_{ws} = c_w F$ as $1/(1-M^2)$.

(c) The corrections due to the model displacement are, for small Mach numbers, estimated according to equations (3) and (6), as long as it is assumed that along the body contour the assumptions of the Prandtl principle are satisfied with sufficient accuracy. The corrections increase as $1/(1-M^2)^{3/2}$. If at high Mach numbers in the neighborhood of the model the Prandtl principle no longer holds, the correction velocity at the tunnel center is obtained from the additional velocity measured at the wall above and below the model with the aid of equation (4) and the factor m given in table 2. From the additional velocity measured at the wall, the part due to the drag is to be subtracted as this correction is already taken into account. In addition, the effect of the mounting is naturally to be taken into account as is done most simply by a calibration measurement.

At high Mach numbers the previously given corrections depend on measurements that are obtained at a large distance from the model and that there have the same values as in the neighborhood of the model. Because the assumptions for the Prandtl principle used in these corrections are well satisfied at a large distance from the model, the previous corrections are also admissible when the Prandtl principle in the neighborhood of the model no longer holds.

3. Sample Computations and Comparison with the Approximate

Computations of Ferri and Lamla

For the velocity correction due to the model displacement the previously derived equations give higher approximations than those of Ferri or of Lamla. In order to obtain an idea of the admissibility of the assumptions of Ferri or Lamla it is therefore convenient to compare, with the aid of a few examples, the various approximate computations. (See table 3.)

From the comparison of the values in the table it is seen that, in accordance with expectation, the wind-tunnel corrections of Ferri are greatly overestimated. The values of Lamla, particularly for the tunnel with open section, also still lie considerably higher than the more accurate values of Franke-Weinig or Glauert-Gothert.

The comparison of the closed circular tunnel with the closed tunnel with plane walls shows that in spite of the same ratios of model thickness to tunnel height the wind-tunnel corrections considerably deviate from each other.

4. Relations from the Adiabatic Equation as an Aid to Wind-Tunnel Corrections

For the correction of dynamic pressure and Mach number, several of the relations obtained from the adiabatic equations are of importance. These are:

Correction of the dynamic pressure:

$$dq/q = (2-M^2) \quad dv/v = -1/2 (2-M^2) \quad dp/q$$

Correction of the Mach number:

$$dM/M = (1 + \frac{k-1}{2} M^2) \quad dv/v = -1/2 (1 + \frac{k-1}{2} M^2) \quad dp/q$$

where

p static pressure

q $\rho v^2/2$, dynamic pressure

v velocity

k 1.405 for air

The value of the expression in parenthesis $(1 + \frac{k-1}{2} M^2)$ is represented in figure 12. The factors $\sqrt{1-M^2}$, $1-M^2$ and $(1-M^2)^{3/2}$, which occur frequently, are also plotted in figure 13.

VII. COMPARISON OF THE COMPUTED CORRECTIONS WITH

WIND TUNNEL CORRECTIONS

To check the tunnel corrections determined above for high subsonic velocities, the high-speed DVL wind tunnel was available. This wind tunnel has a closed measuring section of 2.7-meter diameter and attains at about 50 percent of the available driving power the velocity of sound in the measuring section.

1. Changes in the Wall Pressure through the Mounting of

Rectangular Wings of Various Chords

In order to learn the effect of the tunnel wall on the measurement values at high subsonic velocities, four rectangular wings of

equal profile, NACA 0015-64, with various chords were investigated in this tunnel; the chords were $t = 350, 500, 700$ and 1000 millimeters. The span ($B = 1.35$ m) and the mounting were the same for all four wings investigated. The additional velocities produced by the tunnel walls cannot be directly measured. At most the increase in the surface pressure at various Mach numbers could be compared insofar as the change in the surface pressures in the free air stream at high subsonic velocities could be considered as known from some computations. In this case too, however, the observed increase in the surface pressure is due partly to the increase of the flow about the profile as a result of the compressibility effect and partly to the effect of the tunnel wall, so that the part due to the wall effect, obtained through splitting the measured values, is at least uncertain.

A useful method of checking the corrections is offered, however, by the measurement of the wall pressure in the model plane. The computation of the wall pressure depends on the same assumptions as the computation of the correction velocities at the tunnel center, as has already been explained in the previous sections. This close connection expresses itself also in the fact that the pressure changes due to the model measured at the wall stand in quite definite relation to the correction velocities at the center of the tunnel. (See equation 4.) In addition, the pressure changes at the tunnel wall are always greater than the pressure changes entering the correction computation so that the wall pressures are more easily susceptible to an accurate measurement. The tests were conducted by measuring the wall pressures p_I , p_{III} , and p_w for various dynamic pressures. (See fig. 14.) The measuring stations for the pressures p_I and p_{III} were uniformly distributed over the entire circular cross-section. For the measurement of p_w in the test section, three close-lying holes were bored in the wall in the model plane above and below the model and these were combined to give the arithmetic mean. It may be shown that the dynamic pressure and the Mach number in the plane of the model and the wall pressure p_w without the model were functions only of the ratio $(p_I - p_{III})/p_I$. These relations were determined by tests and plotted as calibration curves. The values determined from this ratio for the dynamic pressure and the Mach number are, in what follows, denoted as the uncorrected test-section values. If a model is mounted in the test section, the indicated wall pressure p_w changes for equal pressure ratio $(p_I - p_{III})/p_I$. From this change of the wall pressure, the corrections to be applied can be determined.

The wall-pressure changes measured for wings of various chords are plotted in figure 15 as functions of the corrected Mach number in the test-section center. In order to eliminate the effect of the mounting, the wall-pressure change was not referred to the wall pressure of the free test section but to the wall pressure for a mounted wing

of 350-millimeter chord. In order to obtain a computational comparison the Prandtl principle was assumed to be valid also in the neighborhood of the model. Although this assumption does not hold with certainty if compression shocks occur at the model, that is, at a Mach number above approximately 0.76, it may nevertheless be assumed that the admissibility of the assumptions can be checked from the trend of the computed and measured curves. This assumption holds at least for the greater part of the curve, which is below the critical Mach number of 0.76. The computation of the wall-pressure changes was then carried out with the aid of equations (3), (5), (6), and (7) and tables 1 and 2, first without taking account of the measured wing drag and again with the drag taken into account. It was found that for the wings investigated, the wing drag becomes of significance only if it has increased greatly because of the compression shock. Nevertheless it even then has a small effect so that the error in taking account of the wing drag has not too great an effect on the curves.

The effective Mach number with which the rise in the wall pressure is to be computed is not unique, particularly at high Mach numbers. The Prandtl principle requires that the mean Mach number of the flow field under consideration be substituted. In order to show the effect of this uncertainty, two curves were computed, one for the corrected Mach numbers at the tunnel center, which in any case had to be considered as too small in the neighborhood of the model. For the other curve the Mach numbers computed at the wall were used, which in the neighborhood of the body came close to the mean Mach number. From the curves in figure 15 it is seen that the computed curves on the whole agree well with the measurement points. The existing deviations all lie within a scatter range that can be explained by an inexact estimate of the effective Mach number.

It may therefore be said in conclusion that the computations throughout agree with the measurements to the degree that may be expected from the assumptions made.

With regard to the previously mentioned uncertainty in the determination of the effective Mach number, it is further to be added that this uncertainty does not exist in the correction of the dynamic pressure and the Mach number. The principal factor of importance, namely, the ratio of measured wall-pressure change to the tunnel correction, is independent of the corresponding Mach number. Only in the determination of the correction factors m_{corr}/m and $\tau_{v\text{corr}}/v$ at large model chord and in the taking into account of the wake displacement does the Mach number enter. The deviation of the computation through uncertainties in these corrections should not be of great significance.

2. Effect of the Lift on the Wall Pressure

The measurements described above on the rectangular wing were carried out for a symmetrical flow about the wing, that is, for zero lift. The fact that a change in the angle of attack to a first approximation has no effect on the mean wall pressure is to be expected from the considerations of section II, 2. The circulation due to the lift produces on the upper and lower sides equal and opposite velocity and pressure changes so that the disturbance velocity through the circulation in forming the mean of the wall pressures on the top and under sides drops out. There is only an effect due to changes in the wing drag as a result of different angle of attack, which, however, because of the small effect of the drag on the wind-tunnel corrections, cannot be of great significance.

These facts could be confirmed by tests. Figure 16 shows, for a rectangular wing of 500-millimeter chord, the wall pressure p_w as a function of the pressure difference $p_I - p_{III}$, already discussed previously for 0° and 5° angles of attack. It is seen that there are no systematic deviations between the measuring points of the various angles of attack that could not be ascribed to errors in measurement. The 5° angle of attack means, however, that at high Mach numbers, in general, the limit of the angle of attack is of greatest interest in the wind tunnel experiment. This independence of the angle of attack means a considerable simplification in evaluating the results because the calibration curves for dynamic pressure and Mach number need not be corrected for each investigated angle of attack.

3. Pressure Drop in the Test Section Due to Wake Displacement

In order to check equations (5) and (7) for taking into account the wake behind the drag bodies, use was made of the fact, discussed in section II, 2, c, that at a large distance behind the model the disturbance velocity due to the wake is just twice as great as the corrections at the wing location according to the equation (5). It was further assumed that at the end of the test section, that is, about two wing chords behind the investigated wing of 500-millimeter chord, this final value is already practically attained. Under these assumptions the additional pressure drop due to the wake as compared with the test section without obstacles could be computationally estimated. For the effective Mach number there were again substituted two values which correspond respectively to the Mach number in the test section and the Mach number at the end of the test section.

For this comparison too (fig. 17), the measuring values lie within the region that is described by the computed curves. The residual deviations can be ascribed to measuring errors or deviations in the effective Mach number.

VIII. SUMMARY

(1) For wings with finite ratio of span to tunnel diameter and for bodies of rotation in closed circular tunnels, the wind-tunnel corrections due to the model displacement in an incompressible flow are computed.

The corrections, in contrast to Glauert's method, are given as a function of the volume of the displacing body. In this method the effect of the contour shape for slender body shapes becomes vanishingly small; in particular in the limiting case of very slender bodies the same form factor is obtained for three-dimensional and two-dimensional flows.

(2) For incompressible flow the additional velocities due to the dead-water region behind the resistance bodies is represented by a simple equation.

(3) With the aid of the Prandtl principle it is shown that for compressible flow the tunnel corrections due to the model displacement increase as $1/(1-M^2)^{3/2}$ and due to the wake for equal drag area as $1/(1-M^2)$. The corrections due to the lift remain, for equal lift coefficient, unchanged provided the wing chord is small compared to the tunnel height.

(4) On increasing the Mach number the corrections to take account of the stream curvature for models with large chord rise as $1/\sqrt{1-M^2}$ so that these corrections have significance at high Mach numbers even though they are negligible at small Mach numbers.

(5) The derived corrections for high Mach numbers remain valid if along the model surface the assumptions of the Prandtl principle are no longer satisfied. The limiting Mach number up to which the method is applicable is to be determined by wind-tunnel tests.

(6) A comparison between computation and measurement shows good agreement as far as may be expected from the assumptions made.

Translated by S. Reiss
National Advisory Committee
for Aeronautics

TABLE I - FACTOR τ_V FOR THE CLOSED CIRCULAR TUNNEL¹ (EQUATION 3)

[B, span of rectangular wing; D, tunnel diameter]

Model shape	Body of rotation	Rectangular wing			
		B/D = 0	B/D = 0.25	B/D = 0.50	B/D = 0.75
Factor τ_V	1.02	1.02	1.04	1.06	1.10

¹Glauert (reference 3, p. 58) gives for the factor τ_V after suitable conversion for bodies with rotational symmetry:

$$\tau_V = 0.797 \times 4/\pi = 1.016$$

for closed circular tunnel,

$$\tau_V = -0.206 \times 4/\pi = -0.263$$

for open circular tunnel. The deviations of these values from those in table 1 lie within the accuracy of computation.

TABLE II - FACTOR m FOR THE CLOSED CIRCULAR TUNNEL (EQUATION 4)

[B, span of rectangular wing; D, tunnel diameter]

Model shape	Body of rotation	Rectangular wing		
		B/D = 0	B/D = 0.25	B/D = 0.50
Factor m	0.45	0.45	0.46	0.49

TABLE III - VELOCITY CORRECTION IN VARIOUS WIND TUNNELS FOR
 A WING WITH ELLIPTICAL CROSS-SECTION WITH $d/t = 0.10$
 FOR A MACH NUMBER OF 0.75

Tunnel shape	$\frac{\text{Wing thickness}}{\text{Tunnel height}}$ (percent)	$\frac{\text{Span}}{\text{Tunnel width}}$	Velocity correction (percent)
Closed tunnel with parallel walls; $h = \text{constant};$ $b \rightarrow \infty$	4	1	11.4 -- Ferri 4.2 -- Lamla 2.5 -- Franke- Weinig and Glauert- Göthert
Open free jet with parallel walls; $h = \text{constant};$ $b \rightarrow \infty$	4	1	-4.2 -- Lamla -1.3 -- Glauert- Göthert
Closed circu- lar tunnel	4	0.25	1.2 -- Göthert

REFERENCES

1. Ferri, A.: The Guidonia High-Speed Tunnel. Aircraft Engineering, vol. XII, no. 140, Oct. 1940, pp. 302-305.
2. Lamla, E.: Der Einfluss der Strahlagrenze in Hochgeschwindigkeits-Windkanälen. F.B. 1007, Luftfahrtforschung, Dez. 15, 1938.
3. Glauert, H.: Wind Tunnel Interference on Wings, Bodies, and Airscrews. R. & M. No. 1566, British A.R.C., 1933, pp. 54-58.
4. Franke, A., and Weinig, F.: The Correction of the Speed of Flow and the Angle of Incidence Due to Blockage by Aerofoil Models in a High Speed Wind Tunnel with Closed Working Section. F.B. 1171, Rep. & Trans. 259, British M.A.P., April 1946.
5. Fuchs, Richard, und Hopf, Ludwig: Handbuch der Flugzeugkunde, Bd. II. Aerodynamik. Richard Carl Schmidt & Co. (Berlin), 1922.
6. Lamb, H.: The Hydrodynamic Forces on a Cylinder Moving in Two Dimensions. R. & M. No. 1218, British A.R.S., 1929.
7. Muttray, H.: Ueber die Anwendung des Impulsmessverfahrens zur unmittelbaren Ermittlung des Profilwiderstandes bei Windkanaluntersuchungen. GDC 10/107T, ZWB Rep. 824/2, Nov. 15, 1937.
8. Lotz, J.: Korrektur des Abwindes in Windkanälen mit kreisrunden oder elliptischen Querschnitten. Luftfahrtforschung, Bd. 12, Nr. 8, Dez. 25, 1935, S. 250-264.
9. Göthert, B.: Einige Bemerkungen zur Prandtl'schen Regel in Bezug auf ebene und räumliche Strömung. (ohne Auftrieb), F.B. 1165, Institut für Aerodynamik, Berlin-Adlershof, Dez. 30, 1939.
10. Prandtl, L.: General Considerations on the Flow of Compressible Fluids. NACA TM 805, 1936.

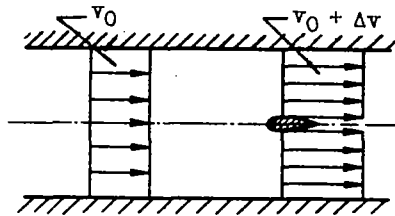


Figure 1. - Wind tunnel with model. One-dimensional velocity distribution according to Ferri.

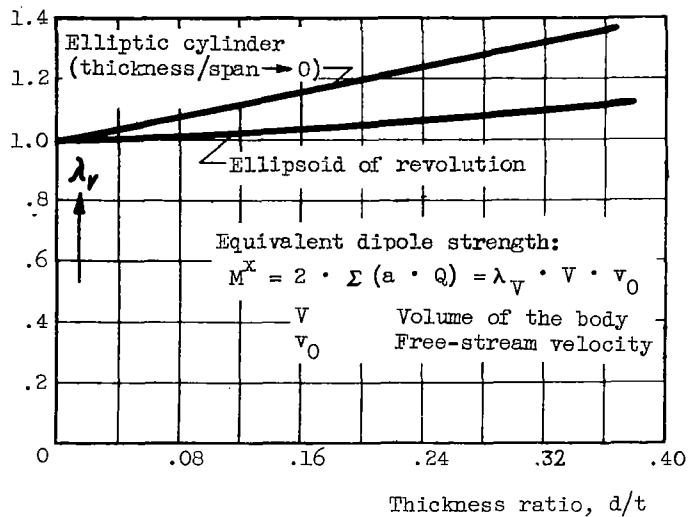


Figure 2. - Equivalent dipole strength for elliptical cylinder and ellipsoid of revolution (recomputed from reference 3).

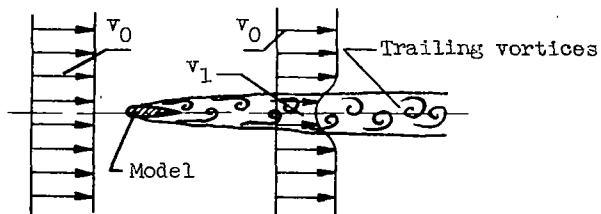


Figure 3. - Model with vortex wake.

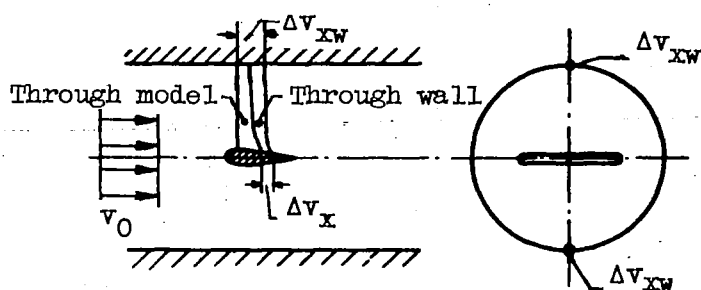


Figure 4. - Velocity distribution for a model in the wind tunnel.

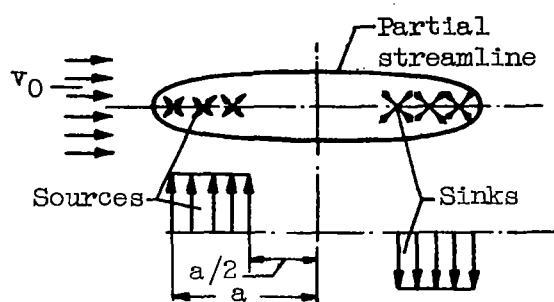


Figure 5. - Distribution of the sources and sinks for the bounding streamlines under consideration.

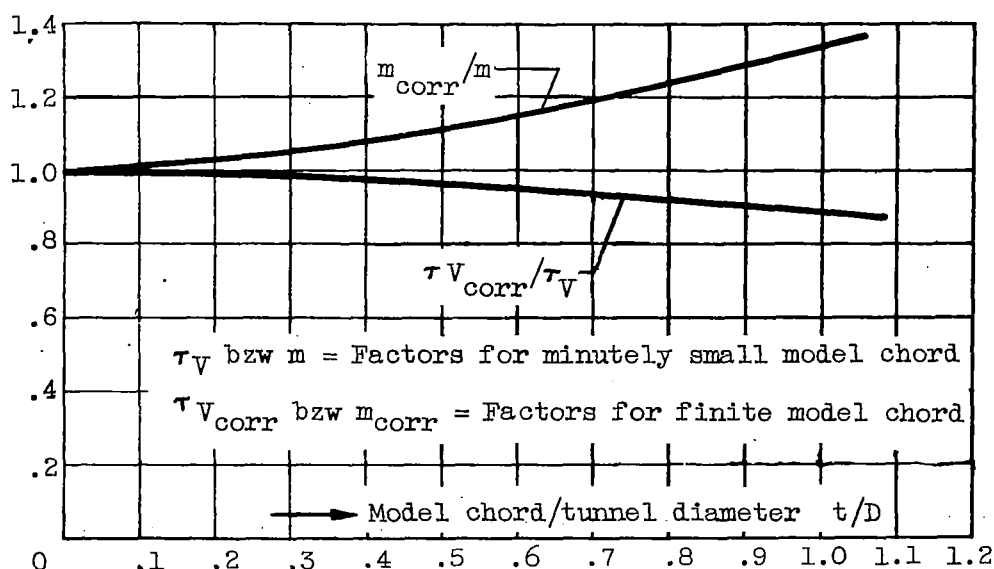


Figure 6. - Effect of the model chord on the factors τ_V (equation (3)) and m (equation (4)) for source-sink body with ratio $F/d \times t = \sim 0.75$ (rotational symmetry or wing with ratio of span/tunnel diameter $\rightarrow 0$).

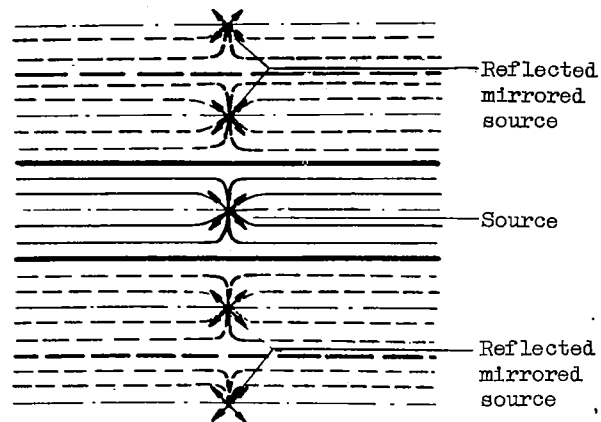


Figure 7. - Source in the tunnel with reflected sources.

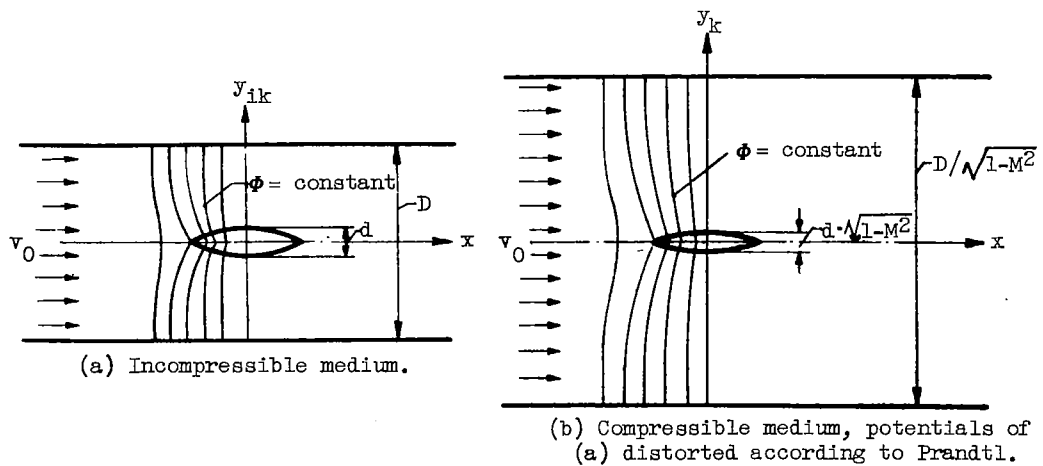


Figure 8. - Wing in closed tunnel for incompressible and compressible flow according to the Prandtl principle.

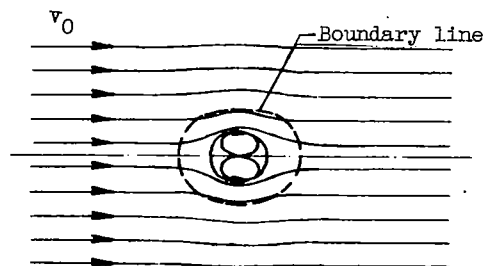


Figure 9. - Dipole in parallel flow.

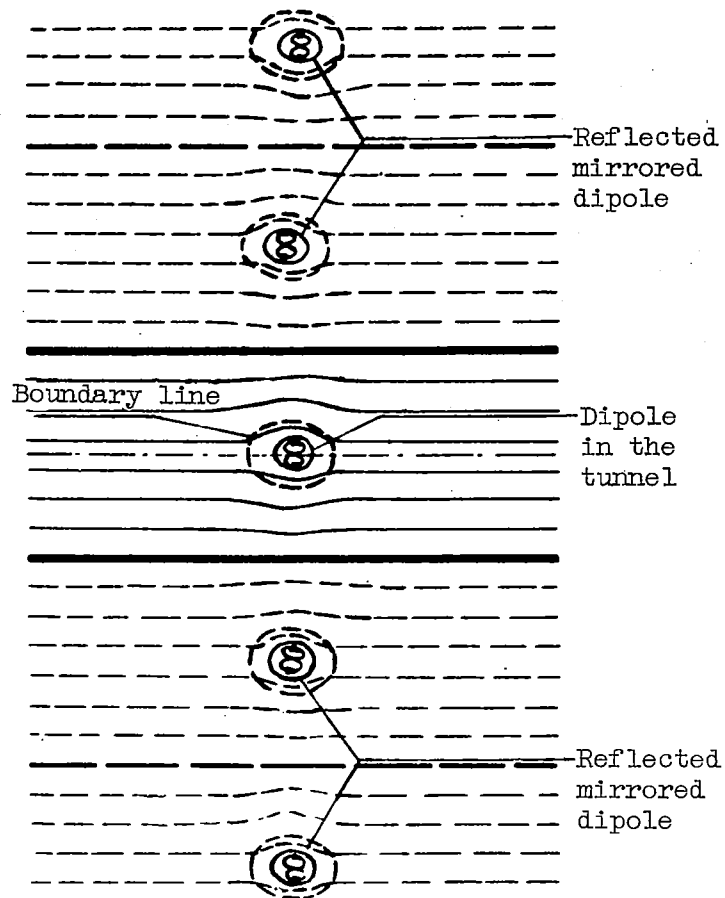


Figure 10. - Dipole in tunnel with boundary lines for the case of the validity of the Prandtl principle.

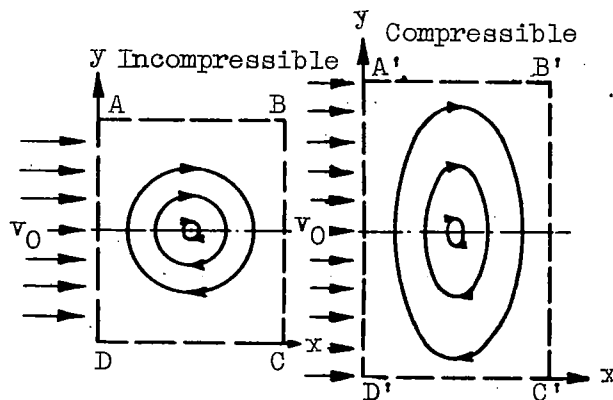


Figure 11. - Potential vortex in the parallel flow.

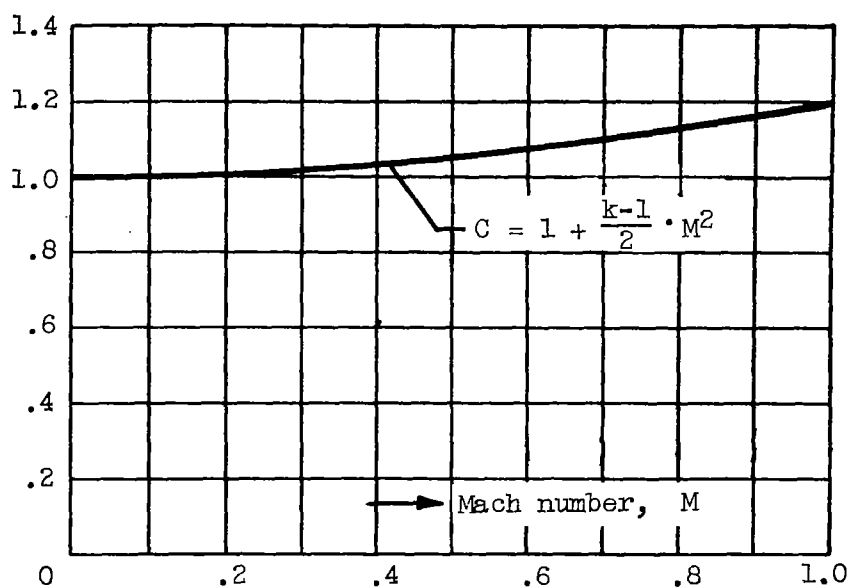


Figure 12. - Factor C as a function of the Mach number.

$$\frac{dM}{M} = C \cdot \frac{dv}{v} = -\frac{1}{2} \cdot C \cdot \frac{dp}{\rho} \frac{1}{v^2}$$

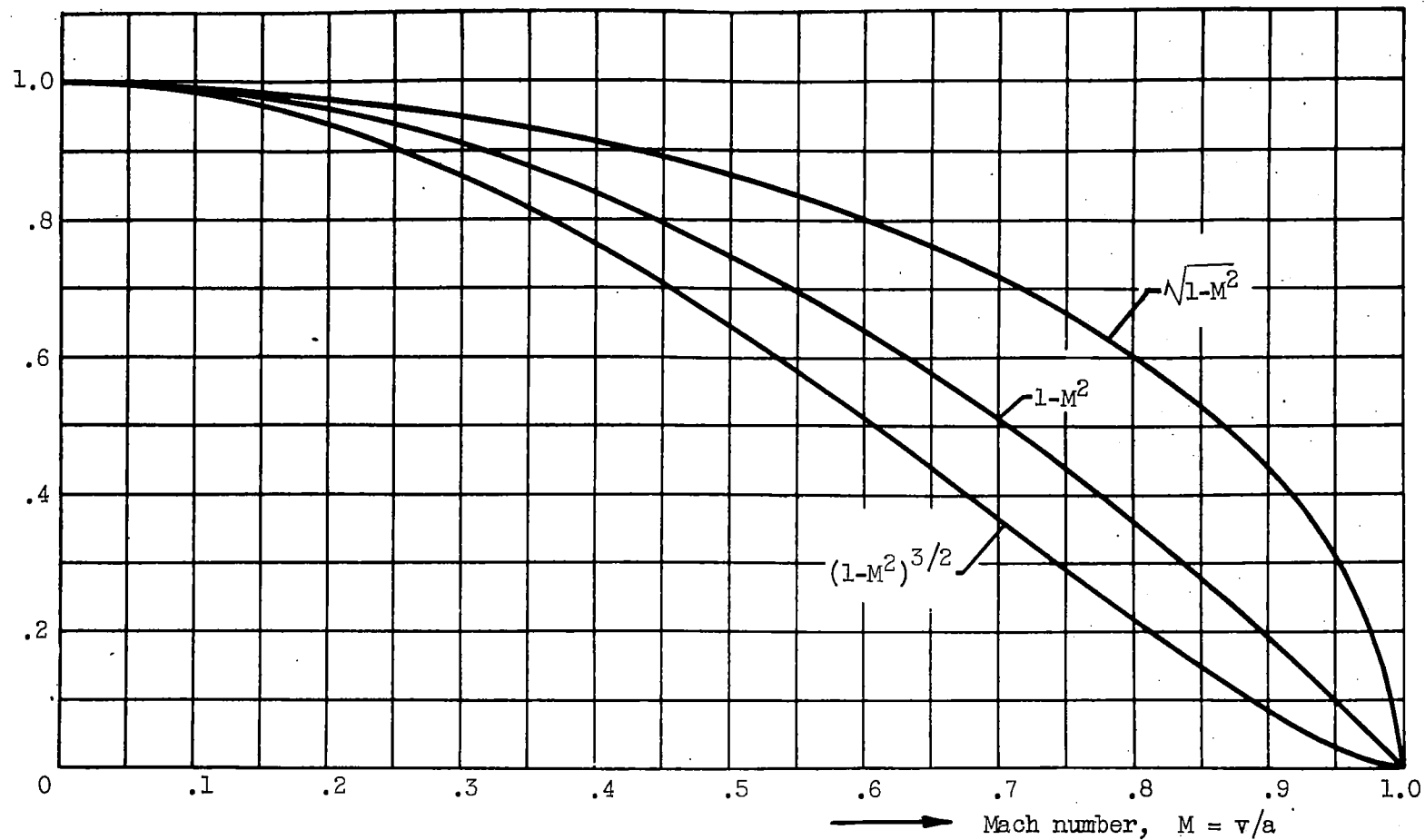


Figure 13. - Values of $\sqrt{1-M^2}$, $1-M^2$, and $(1-M^2)^{3/2}$ as a function of the Mach number.

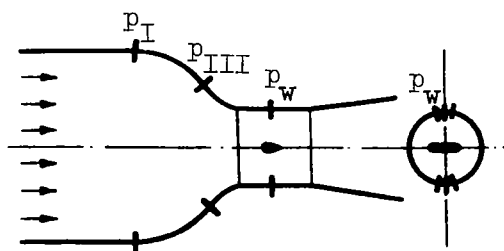


Figure 14. - Wall pressures for determining the dynamic pressure.

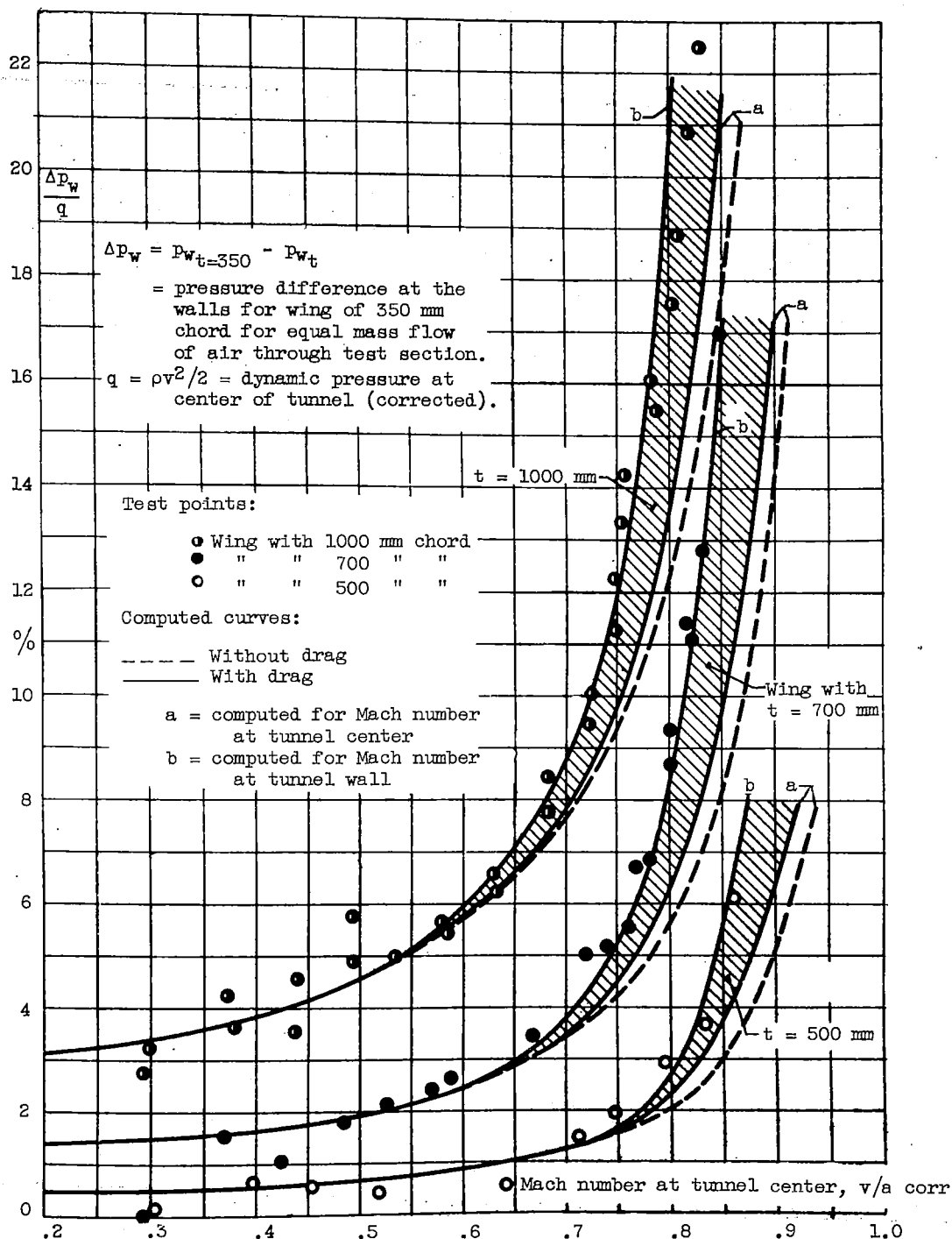


Figure 15. - Comparison of the computed and measured wall-pressure changes through mounting of rectangular wings (NACA 0015-64) with various chords.

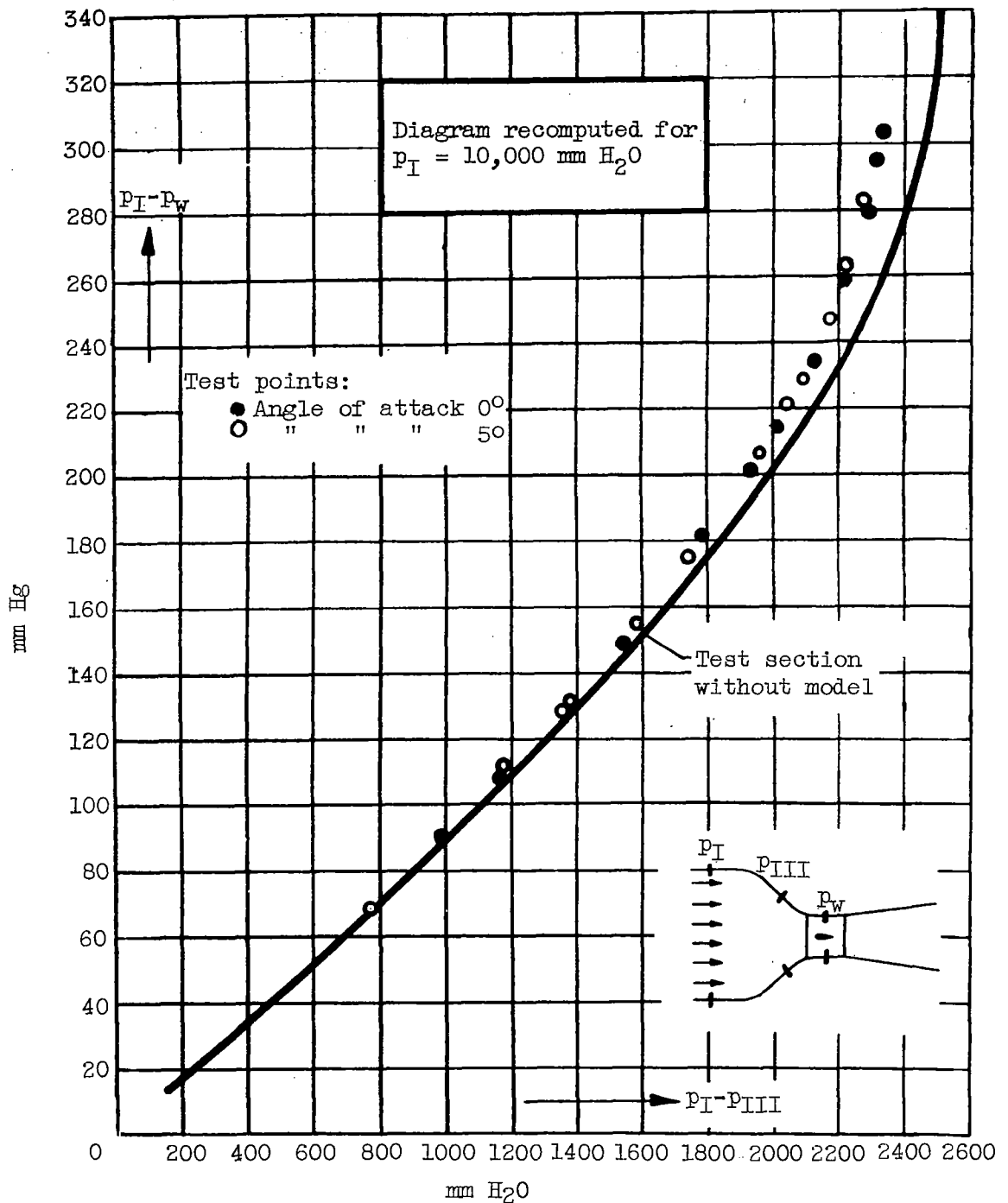


Figure 16. - Wall pressures at the measuring section at 0° and 5° angles of attack of a rectangular wing (NACA 0015-64) with 500-millimeter chord.

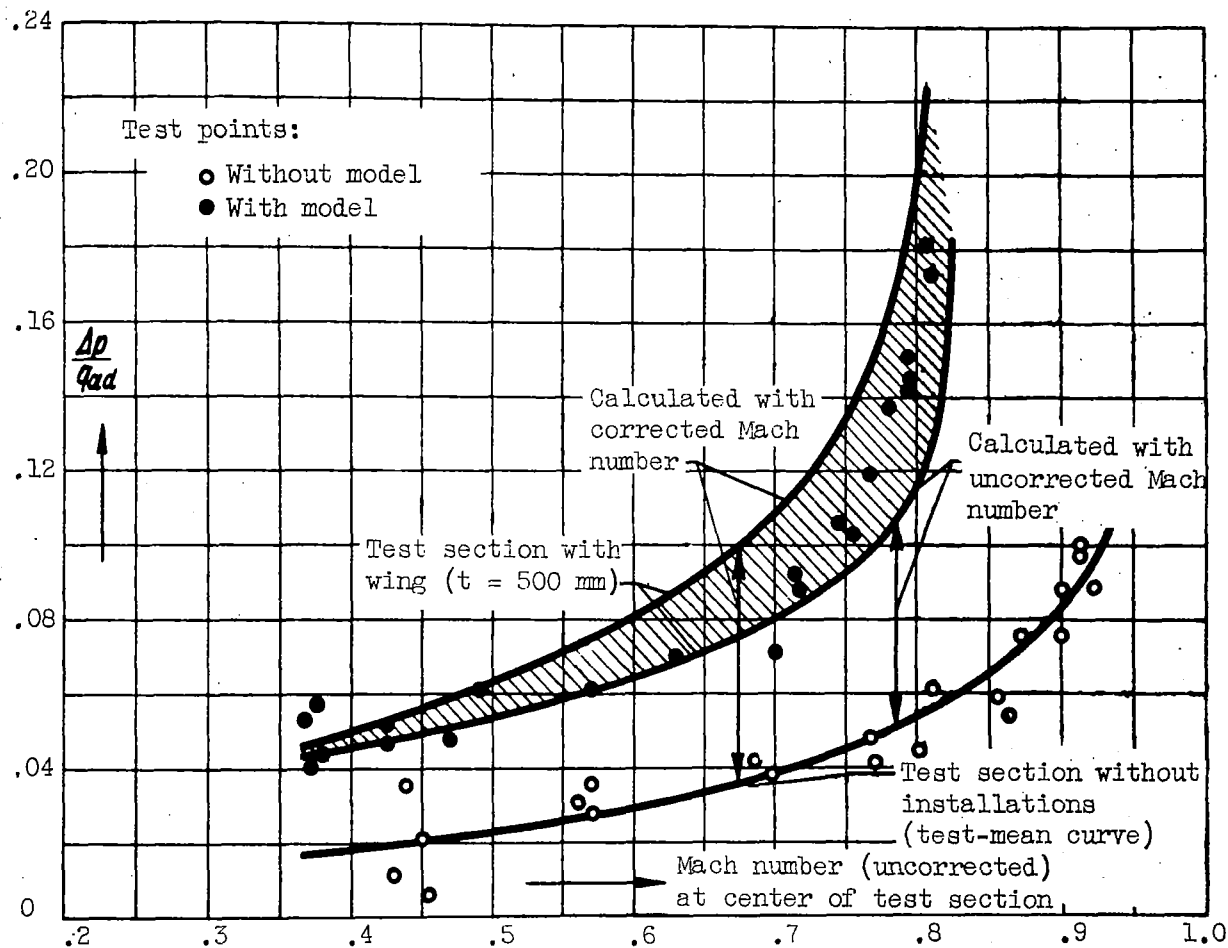


Figure 17. - Pressure drop Δp in the test section with and without the model.
 $\Delta p = P_{init} - P_{fin}$ = wall-pressure difference between the beginning and end of the test section.
 $q_{ad} = P_{tot} - P_M$ = adiabatic dynamic pressure at the center of the test section.